The internal NHS52S04 pullup must be enabled to read the state of the switch. Time must be allowed for the charging of capacitance on this net. NXP indicates the pullup could be as high as 62k Ohms at 1.85V. This is a time constant of 102uS=62K*1500pF*1.1(10%). SW should wait 0.3mS (three time constants) after enabling the pullup to insure an accurate reading.

6.2.14 RF Design

6.2.14.1 General Description

The NHS52S04 has an integrated BLE radio, a protocol stack and application profile. The SOC can support master and slave modes concurrently. This was an important feature to support for the future Pod's generations. The RF module is supplied through its LDO mode (instead of DC-DC) to reduce the cost and size of additional components. Also, the RF radio has a higher Rx sensitivity (-95dBm) in LDO mode in comparison to the -94dBm in DC-DC mode.

The radio Tx power is software configurable between -28dBm to +6dBm with an output error of ± 1.5dBm (@2dBm, TXM1 mode). Currently, the max software setting is +2dBm. This helps to save power making it more consistent with the Omnipod 5-SAW product. The NHS52S04 has an integrated balun, which also helped reduce the size and cost of additional.

The following parameters of the BLE radio have been examined: return loss, bandwidth, insertion loss and radiation pattern.

6.2.14.2 Antenna Type

The type of antenna used for the OmniPod 5 Orion Pod PCB (PT-001690) is an Inverted F (Inv-F) type PCB trace antenna. This is the same antenna design used on the OmniPod 5 SAW Pod PCB (PT-000541). A screen capture of the OrCAD design of the OmniPod 5 Orion PT-001690 Inv-F antenna is provided below in Figure 4.

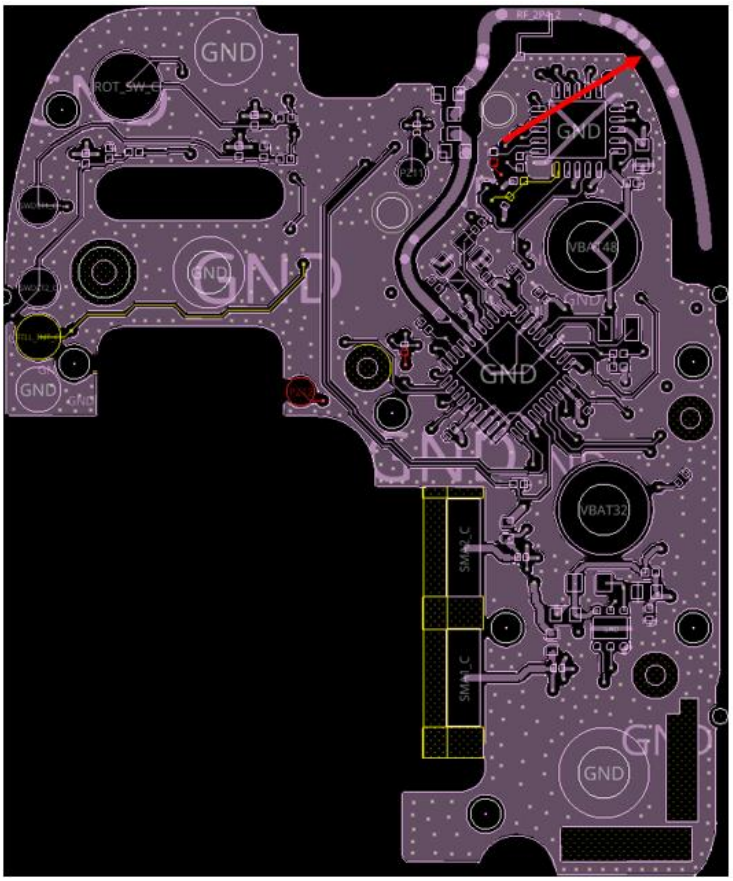

Figure 4: PCB design of the OmniPod 5 Orion PT-001690 Inv-F PCB trace antenna.

PCB trace antennas are two-dimensional (2D) structures that are on the same plane as the PCB. The PCB antenna has the advantages of cost reduction and ease of manufacturing. The Inv-F PCB trace antenna is a compact design that provides a minimal footprint and better rejection of detuning effects from proximity to the human body, as shown in early simulations.

The Inv-F antenna design was chosen over the loop antenna for three primary reasons. First, the Inv-F antenna has an overall better gain and radiation pattern than the loop antenna that is currently employed in other Pod versions such as EROS, DASH and SAW-DASH. Second, the on-body radiation efficiency of the Inv-F antenna is ~15%, which is better than the loop antenna's on-body radiation efficiency of ~10%. The improved radiation efficiency of the Inv-F antenna means that more energy is transmitted to a potential receiver than for the loop antenna. Third, the Inv-F has more consistent return loss performance than the loop antenna, meaning it is less sensitive to changes inside and outside of the Pod than the loop antenna. Overall, these parameters result in improved Pod-to-PDM communications over the loop antenna while not sacrificing Pod-to-CGM communication performance.

Another important design consideration for the antenna was the matching and filtering components. Both the OmniPod 5 (41104) and Dash (18048) Pods use the loop

antenna design. The antenna layout utilized in the OmniPod 5 Orion PT-001690 PCBA population is of similar design as the Dash (18048) population, but with an improved antenna match. Independent testing of the antenna following Dash development showed that the OmniPod 5 population provided an additional 3dB to 4dB of peak power.

6.2.14.3 Harmonic Filter

The OmniPod 5-SAW (PT-000541) and the OmniPod 5 Orion (PT-001689) PCBAs contain the same harmonic filter because the Inv-F antenna is a linear antenna, meaning that it is a good radiator at it centers frequency and increases harmonics. For OmniPod 5 Orion, the Harmonic Filter consists of components C11, C14 and L1. Test prove that the harmonic filter improves the Inv-F antenna gain at the desired center frequency of 2.44GHz. Note, that since the OmniPod 5-SAW and OmniPod 5 Orion PCBAs have the same antenna and Harmonic Filter designs, the following simulation data is applicable to both platforms.

6.2.14.4 Inverted-F Antenna Simulated In-Air Performance

To evaluate the Inv-F antenna design, simulations were performed. All simulations were performed using HFSS, a three-dimensional (3D) full-wave solver from ANSYS©. The radiation gain pattern of the antenna can be seen in Figure *5*. The results are obtained in simulation without human body torso model, thus the off-body pattern. The 2D and 3D patterns are shown in Figure *5* for three orientations of the Pod, corresponding to three cross-section planes: XY, XZ, and YZ.

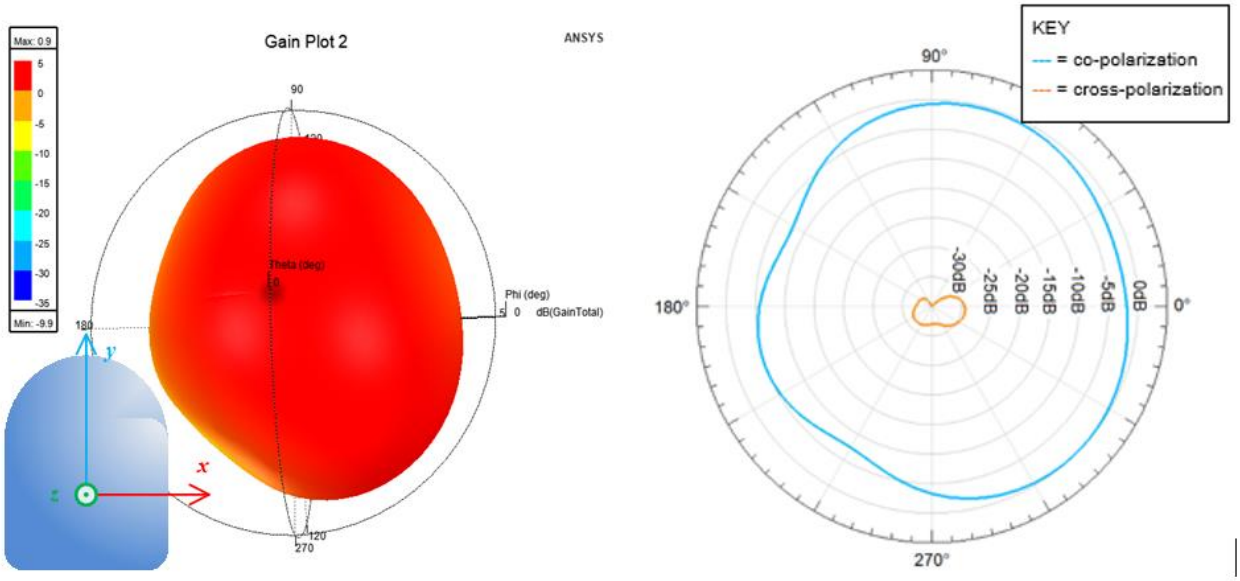
Gain Plot 2
ANSYS
Max: 0.9
Min: -9.9
Theta (deg)
Phi (deg)
dB(GainTotal)
KEY
= co-polarization
= cross-polarization
90°
180°
0°
270°
-30dB
-25dB
-20dB
-15dB
-10dB
-5dB
0dB

(a)

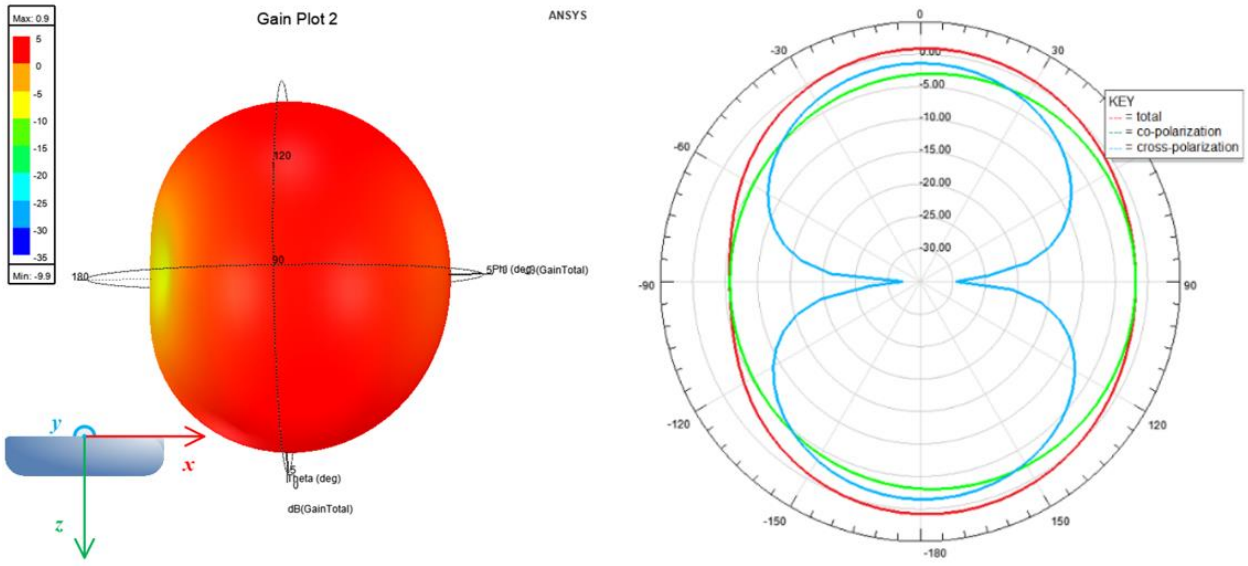
Gain Plot 2
ANSYS
Max: 0.9
Min: -9.9
Theta (deg)
Phi (deg)
dB(GainTotal)
KEY
= total
= co-polarization
= cross-polarization
-5.00
-10.00
-15.00
-20.00
-25.00
-30.00

(b)

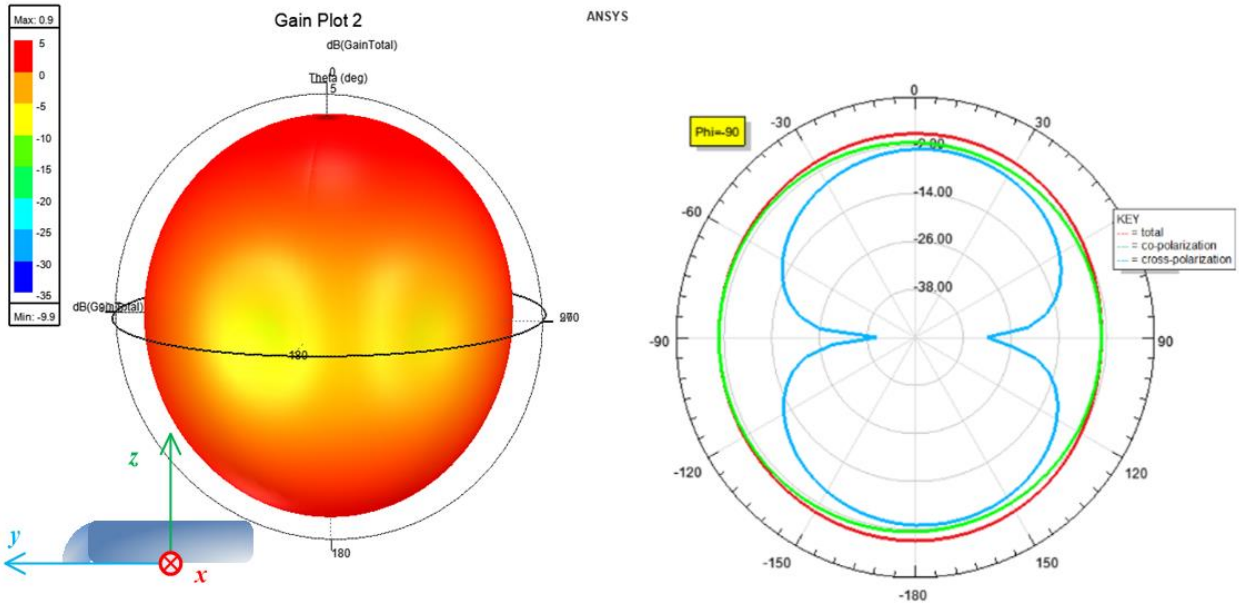

(c)

Figure 5: Simulated gain patterns for the OmniPod 5 PT-000347 Inv-F antenna.

(a) In-plane (XY) with the OmniPod 5 PCB results: 3D (left) and 2D (right). Strong parallel polarization in the PCB plane is observed while cross-polarization is over 20dB weaker.

(b) XZ plane results: 3D (left) and 2D (right). The antenna shows strong broadside radiation at both polarizations.

(c) YZ plane results: 3D (left) and 2D (right). Excellent omni-directivity present in the YZ plane cross-section.

The simulated radiation pattern shows the maximum gain is at 0.9dBi, which is comparable to the preliminary measurement results at 1.1dBi. Strong parallel to perpendicular polarization ratio is seen in-plane with the board.

The simulation also shows that the maximum antenna radiation efficiency is at 75% across the band of interests. This may be due to simulation error and insufficient distancing between the antenna trace and its ground plane. Further improvement should focus on improving the radiation efficiency. Improvements may be made by increasing the distance between the antenna and ground plane, opening the solder mask around the Inv-F antenna area, and adjusting the Inv-F geometry itself to increase the antenna gain.

6.2.14.5 Inverted-F Antenna Simulated On-Body Performance

Although the in-air simulation results provide insight into the behavior of the antenna, the actual use case of the Pod is with the antenna close to the human body. When the antenna is placed on the human body, the body affects the antenna parameters such as tuning and radiation pattern. Therefore, it is important to simulate the antenna performance on a body model to determine the Pod's use-case performance. An image of the human torso model used for simulations is provided in Figure 6.

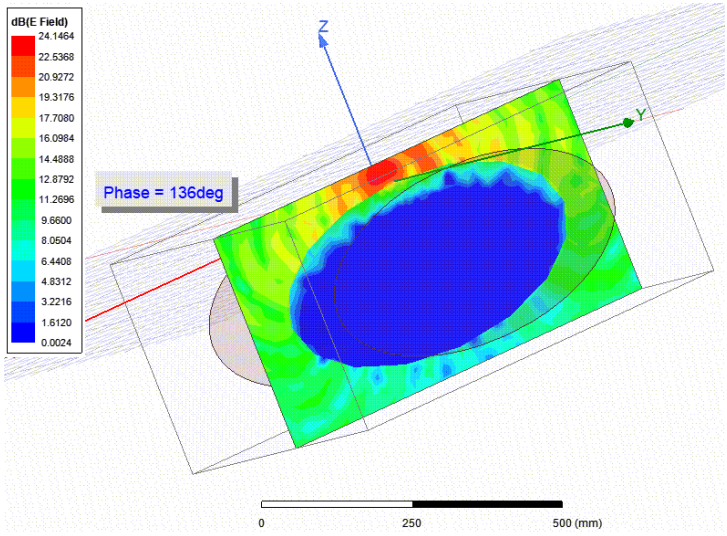

Figure 6: Human torso model used in on-body antenna simulations. The torso (transparent gray elliptic cylinder) is encased in an air box. The colors indicate the strength of the electric field at those locations in space if the Inverted-F antenna were placed at the origin of the XYZ coordinate system.

Figure 6 also provides an overlay of the electric field generated by the Inv-F antenna when the antenna is located on the “stomach” of the human torso model. This simulated electric field strength shows that if a receiver (e.g. the CGM) were placed on the opposite side of the torso (i.e. the back), communications between the Inv-F antenna and the receiver would not be established by waves traveling through the body, but by waves traveling along the surface of the human body.

The radiation gain pattern of the antenna when mounted on a human body torso model can be seen in Figure 7 below. The 2D patterns are shown for three orientations of the Pod, corresponding to three cross-section planes: XY, XZ, and YZ.

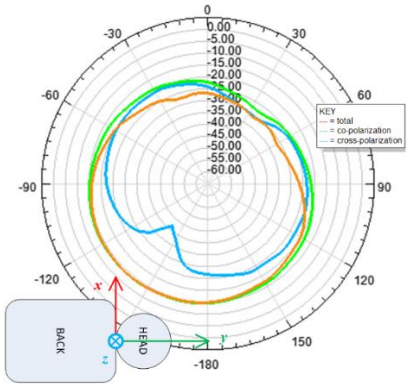

(a)

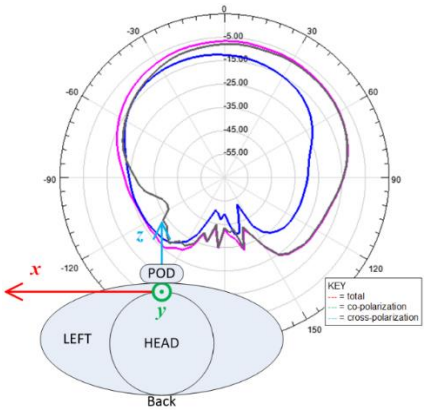

(b)

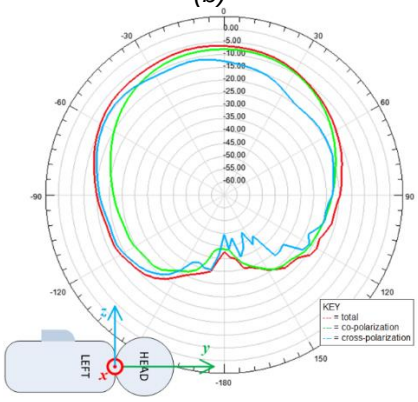

(c)

Figure 7: On-body simulated results for the Inverted-F antenna.
(a) Gain plot in the XY plane. (b) Gain plot in the XZ plane. (c) Gain plot in the YZ plane.

The simulated results are comparable with the preliminary measurement results from an external contacting partner, RF2B, although the simulated gain results are lower than the measured. The radiation efficiency decreases to about 15% when attached to this human torso model. This may not be the most representative of reality because the torso model is configured among the most lossy models, and the PCBA is so closely attached to the torso model that the tight clothing case is represented. However, learning about the limiting case helps to design for the worst case and guarantees robust RF link in all cases.

6.2.14.6 Antenna Return Loss and Bandwidth

The return loss of an antenna is a measure of the effectiveness of the matching to a 50Ω transmission line. While the QN908x's RF port is not a perfect 50Ω impedance, NXP's performance claims are based on a 50Ω load, as is common in the RF design. A mismatched antenna produces high return losses, indicating that energy is reflected rather than transmitted – an undesirable situation for an antenna at its intended operating frequency. The S_{11} parameter, which describes the return loss in terms of power ratios, is calculated using the equation below.

$$S_{11}\,[dB] = 10\log_{10}\left(\frac{P_{incident}}{P_{reflected}}\right)$$

It is worth noting that although the terms "return loss" and the "S_{11} parameter" are used interchangeably, there is a slight difference. Return loss is typically used in relation to voltage measurements and ratios while the S_{11} parameter is used in relation to power ratios. That being said, this distinction is not carried through this document, and both return loss and S_{11} here refer to system measurements in terms of power.

The return loss of the Inv-F antenna in different locations on the human body as measured by a network analyzer are shown in Figure 8 and Figure 9. The measurements were performed with an adult male of 6 feet high and 180lb weight. The return loss curves of the antenna when attached to stomach and thigh are showing sufficient bandwidth well below -10dB level. The antenna return loss is impacted by human body of various types, which must be taken into consideration when viewing any on-body RF measurements. Additionally, the Smith charts show that the antenna is well-matched at Bluetooth frequencies – better so than the loop antenna design.

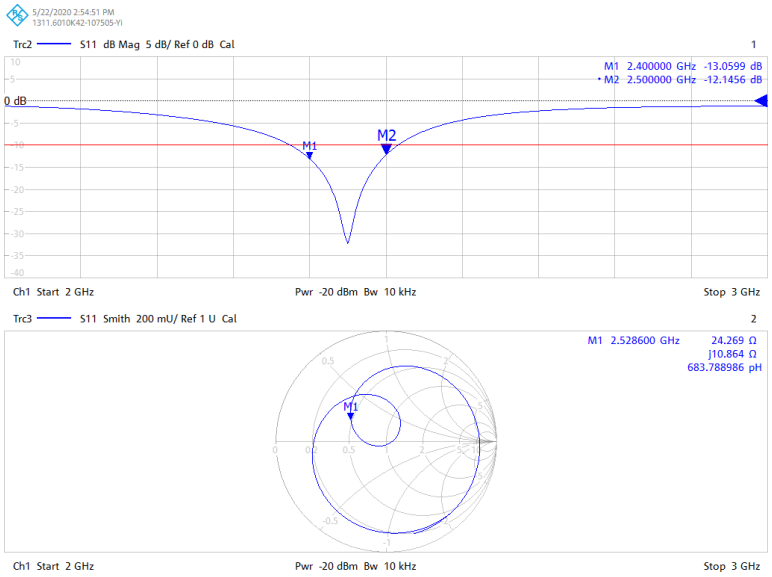

Figure 8: Inverted-F antenna excitation port S_{11} and corresponding Smith chart when Pod is on stomach.

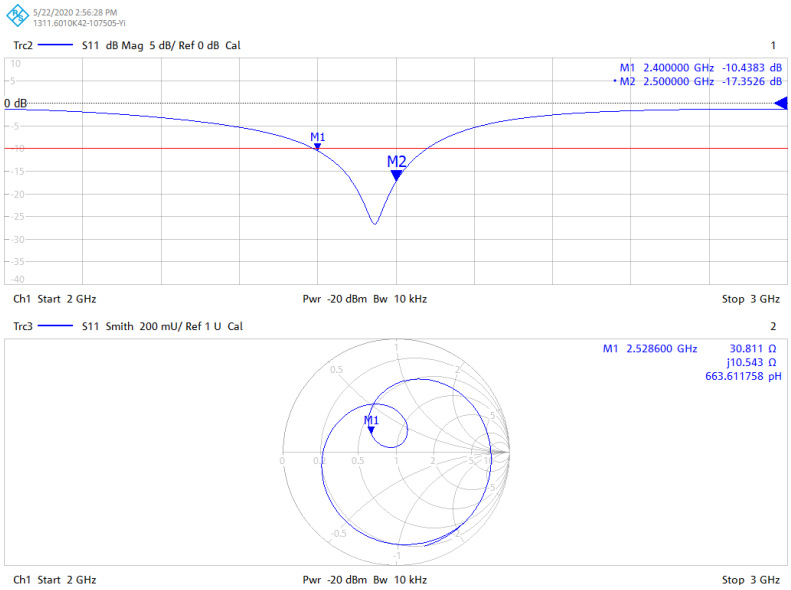

Figure 9: Inverted-F antenna excitation port S_{11} and corresponding Smith chart when Pod is on thigh.

The on-body measurements in Figure 8 and Figure 9 can also be compared to the return loss measurement with the Pod on a workbench. The return loss of the Pod when placed on a workbench is provided in Figure 10.

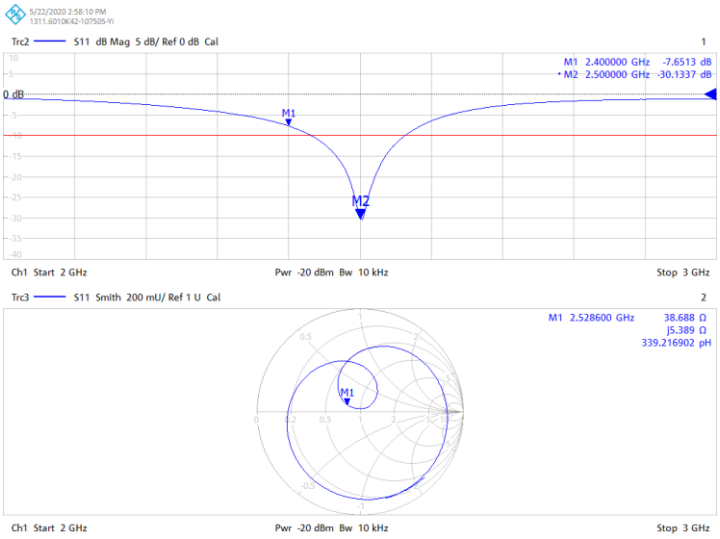

Figure 10: Inverted-F antenna excitation port S_{11} and corresponding Smith chart when placed on a workbench with the bottom facing up.

It can be seen in Figure 10 that the return loss of the Inv-F antenna when placed on a workbench (wood bench equivalent) is not below -10dB threshold across the band of interests. This is acceptable because it actually helps to limit the pairing range, which helps ensure Pods are not incorrectly paired with incorrect PDMs or CGMs.

6.2.14.7 Link Budget Analysis: Pod-to-PDM Communication

Another way to analyze the RF performance of the OmniPod 5 Orion system is using a link budget. A link budget shows what the RF losses are and where they occur in the system. In terms of RF communication, the OmniPod 5 Orion system can be broken into two parts: the Pod-to-PDM communication, described in this section, and the Pod-to-CGM communication, discussed in Section 6.2.14.8.

For the OmniPod 5 Orion system, the worst-case scenario occurs when the Pod and PDM are trying to communicate through-body, i.e. a user holding the PDM in front of him/her when the Pod is located on his back. This scenario is further exacerbated when the user is standing in an open area, such as an ocean, beach or large field, and there are no reflections to help bolster the communications link. In these scenarios, the performance is dominated by the antenna gain toward the back of the Pod wearer, as indicated in Figure 11, over the range between approximately 135° to 225°. The average gain measured there is -30.4dBi.

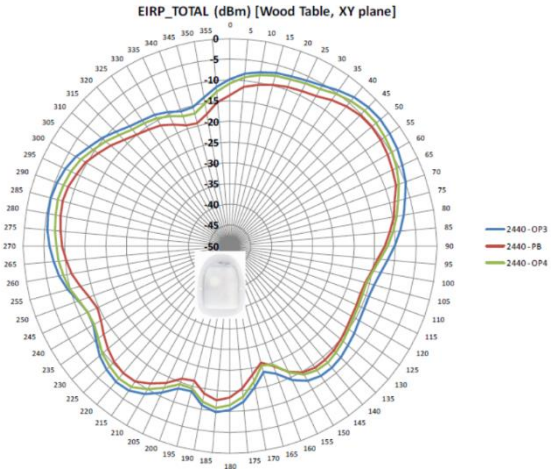

Figure 11: Off-Body EIRP Total (dBm) at 2440MHz per OmniPod 5-SAW

As can be seen in Figure 12, the backward antenna gain of the Inv-F antenna is an average of -27dBi.

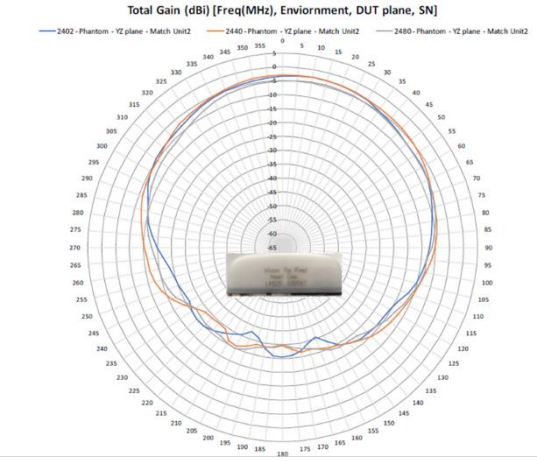

Figure 12: On-body radiation pattern measurement for the Inverted-F antenna

These average gain number is then used to provide an approximation of the RF link performance. Parameters for the link budget calculation when the OmniPod5 Orion system is in its worst-case scenario is summarized in Table 7 below.

Parameter	PDM	OmniPod 5 Pod Orion with Inv-F Antenna
Transmit Power (dBm), P_{TX}	0	0
Receive Sensitivity (dBm), S_{RX}	-95	-95
Antenna Gain (dBi), G_{ANT}	-3	-27
Other Losses (dB)	None	None

Table 7: RF Link Budget Parameters

The parameters in Table 7 are used to calculate the path margin. The equation below shows how to calculate the path margin, assuming that attenuations due to the human body and polarization have already been factored into the values in Table 7.

$$Path\ Margin = P_{TX_{Pod}} + G_{ANT_{Pod}} + G_{ANT_{PDM}} - S_{RX_{G6}}$$

Substituting the knowns in Table 7 into equation above yields a path margin of 65dB for the Inv-F antenna.

Using the path margin, an equivalent through-body range can be calculated via the formula for free space path loss (FSPL), as derived from the Friis transmission formula. This is free-air range beyond the thickness of the human body.

For the Inv-F range calculations, d represents the distance in meters; c, the speed of light in a vacuum in meters per second; and f the operating frequency in Hz, with 2.440GHz for BLE assumed. With these knowns, the following equation can be written as

$$FSPL\ [dB] = 20\log_{10}(d) + 40.2.$$

Additional simplification of for the transmit range of the antenna is shown below (*d)*.

$$d = 10^{\frac{Path\ Margin - 40.2}{20}}$$

Substituting the known values for the INV_F antenna into the equation above yields a transmit range of 17.8m for the Inv-F antenna.

However, the actual antenna performance when worn on body varies dramatically among users. Therefore, the calculated results are typically better than what is physically measured because the actual antenna gain can be much worse than the

measured results on a human body torso simulator. Furthermore, the actual transmit power used in the calculation are measured results out of the chip, not the actual power delivered to the antenna excitation port. Considering how much the antenna excitation impedance can be impacted by human body detuning, the actual transmit power could be a few dB down from the calculated value.

Last but not the least, the calculation shows sufficient communication range for Pod to PDM even when the body is present between Pod and PDM. In common operating cases Pod and PDM are in line of sight with no obstacles, the communication range is expected to be no worse than the calculated results.

6.2.14.8 Link Budget Analysis: Pod-to-CGM Communication

Unlike the worst-case Pod-to-PDM scenario discussed in Section 6.2.14.7, both the Pod and the CGM are mounted on the human body during use. This on-body communication between the two wearable devices are primarily through two wave paths: reflected electromagnetic wave from environment and the surface wave directly travels between the two devices. The reflected waves are environment-dependent, and they can either be very strong when both devices are facing a metallic wall or almost disappear when the user is in an open area like a soccer field. To provide the best user experience, the Pod should be able to communicate to the CGM only through the surface wave propagating around human body surface.

The surface wave propagation model has been studied by researchers and engineers from various organizations worldwide. However, a universal model that is applicable for all different communication devices does not exist, largely because the modeling has to account for many impacting factors including but not limited to operating frequency, antenna characteristics, antenna mounting, and human body differences. In order to model the communication model between the Pod and CGM, thorough experiments must be conducted, and then a statistical model can be built based on the obtained data. This future work is not discussed in this document. Instead, what is provided is an estimation based on the limited available results. Common methods for investigating on-body communication does not utilize the antenna pattern simulated or measured in an anechoic chamber, but directly measure insertion loss between the two antenna excitation ports.

It has been reported that the loss between a monopole antenna near the stomach and a same antenna on the back of the torso is at the level of 50dB. In other words, a 0dBm transmitter would transfer -50dBm power to the receiver. The 50dB is a statistical mean value, and the variation is at the level of 10dB. This result was obtained through measurement over a real person and found comparable to simulation models. The 50dB model was measured with a monopole antenna mounted perpendicular to human body surface. Out of many known antenna types, the monopole antenna has been known as the better coupler between a radiator and the surface wave over human body surface. There are other studies with other types of antennas, but none strictly reflect the behaviors of the Inv-F antenna and the loop antenna. It is although easy to see over 15dB performance degradation for other antennas than the monopole. To author's best knowledge, it is not aggressive to assume an extra 30dB degradation to the Pod-to-CGM communication channel (body front-to-back case) on top of the 50dB model, considering they are both planar trace antennas parallel to human body surface. The

difference between the loop antenna and the Inv-F antenna would require further experiments to investigate.

The above description put 80dB path loss between Pod to CGM, assuming no other obstacles on the path. The rest of the final equation between Pod to CGM would be return loss on both ends, and any thick clothing or objects to lean on that would impact the wave propagation. Therefore, we conclude that the front-to-back use case put Pod to CGM at the boundary of -95dB RF chip sensitivity, with a huge variation in the model due to the statistical nature of the propagation. The Inv-F antenna, though, is expected to perform better than the loop antenna because of higher radiation efficiency and lower return loss.

Future improvement should be looking to change the Pod antenna to other types, for better coupling into the surface wave, and maintain good return loss to maximize the output power from the antenna. It is expected to have 15dB improvement when a new type of antenna is applied to Pod only, leaving CGM as it is today

6.2.15 NH52S04 SOC Power On Reset (POR)

The NH52S04 Hs a Power On Reset circuit which monitors the VBAT_HV supply.

After initial power-up, the POR circuit is disabled to save power. If the application must be protected against supply voltage dips, it must enable one of the brownout detection modules with RESET generation on. When the supply voltage drops below the programmed BOD threshold level, it will allow the reset of the NHS52S04 device. For the NHS52S04, the $V_{th(POR)}$ detection range is between 0.2V and 0.7V.

6.2.16 Brownout Detection (BOD) Device Configuration

The NHS52S04 has two Brown Out detectors which monitors the power supply voltage on the NHS52S04 power supply pins (VBAT_HV or VBAT_LV). The Orion design uses the VBAT_HV BOD. If the supply voltage drops below a configurable voltage threshold level, the BOD sets a flag that can be polled via software or cause an interrupt. The BOD configure API can be used to configure the threshold level. The BOD can also be configured to reset the device over the configuration API. For the NHS52S04, the $V_{th(BOD)}$ detection range is between 1.55V and 3.1V with an accuracy of ± 2.5% (trimmed) or ±7.5% (untrimmed).

6.2.17 NHS52S04 SOC CHIP PACKAGING

The NHS52S04 used in the Orion PCB assembly contains the Quad Flat-Pack (No-leads) (QFN40). A key benefit of the QFP, leadless design is increased PCB space which allows for additional components and/or improved PCB routing options where needed. For details on the QFN40 package, refer to the NHS52S04 Datasheet Rev 1.5, Figures 24 and 25, pages 78 and 79 for details.